Carbon and Hydrogen Isotope Signatures of Dissolved Methane in the Scheldt Estuary

Caroline Jacques[1] · Thanos Gkritzalis[2] · Jean-Louis Tison[1] · Thomas Hartley[1] · Carina van der Veen[3] ·
Thomas Röckmann[3] · Jack J. Middelburg[4] · André Cattrijsse[2] · Matthias Egger[5] · Frank Dehairs[6] · Célia J. Sapart[1,3]

Abstract

We collected water samples from the Scheldt estuary during December 2015 and November 2016 for methane (CH$_4$) concentration and isotopic composition (δ^{13}C and δD values) analyses, to investigate the origin of the excess dissolved CH$_4$, which is a common feature in estuaries. The Scheldt estuary is a eutrophic, heterotrophic tidal estuary, located at the border between Belgium and the Netherlands. The gas chromatography and mass spectrometry analyses revealed (1) variable dissolved CH$_4$ concentrations reaching up to 302.6 nM in surface waters of the Port of Antwerp, which fits within the higher range of values reported for European estuaries, and (2) the presence of surprisingly high isotopic signatures in the upper estuary. While microbial CH$_4$ production dominates in the lower part of the estuary, we observe a clear trend towards isotopically heavier CH$_4$ upstream where isotopic signatures as enriched as −25.2‰ for carbon and +101‰ for hydrogen were measured. We conclude that microbial oxidation of most of the CH$_4$ pool could explain such enrichments, but that the origin of riverine CH$_4$ enriched isotopic signatures remains to be explained. This study identifies peculiar features associated with CH$_4$ cycling in the Scheldt estuary, paving the way for a more thorough biogeochemical quantification of various production/removal processes.

Keywords Dissolved methane · Stable isotopes · Scheldt estuary · Microbial production · Oxidation

Introduction

The distribution of dissolved CH$_4$ in estuaries is governed mainly by riverine inputs, diffusion from the sediments, microbial production in micro-environments, leakage from oil and gas local industries, groundwater discharge, efflux to the atmosphere and microbial consumption (Scranton & McShane, 1991; Middelburg et al., 2002).

Given the complexity of estuarine systems, the relative contribution of these processes to the dissolved CH$_4$ pool is subject to wide spatial and temporal variations (Abril & Borges, 2004).

CH$_4$ produced in anaerobic aquatic environments can be of thermogenic or microbial origin. The two main microbial production pathways are acetate fermentation (see, e.g. Whiticar, 1999):

Communicated by Carolyn A. Currin

✉ Caroline Jacques
caroline.jacques@ulb.ac.be

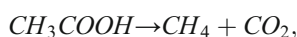1 Laboratoire de Glaciologie, Université libre de Bruxelles, Avenue F.D. Roosevelt 50, 1050 Brussels, Belgium

2 Vlaams Instituut voor de Zee, Flanders Marine Institute, Wandelaarkaai 7, 8400 Ostend, Belgium

3 Institute for Marine and Atmospheric Research Utrecht, Utrecht University, Princetonplein 5, 3584 CC Utrecht, The Netherlands
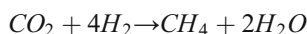
4 Department of Earth Sciences, Utrecht University, Princetonlaan 8a, 3584 CB Utrecht, The Netherlands

5 The Ocean Cleanup Foundation, Batavierenstraat 15, 3014 JH Rotterdam, The Netherlands

6 Analytical, Environmental and Geochemistry Department, Vrije Universiteit Brussel, Pleinlaan 2, 1050 Brussels, Belgium

$$CH_3COOH \rightarrow CH_4 + CO_2,$$

and CO_2 reduction:

$$CO_2 + 4H_2 \rightarrow CH_4 + 2H_2O$$

The determination of CH_4 stable isotope signatures ($\delta^{13}C$-CH_4 and δD-CH_4) has shown high potential to elucidate CH_4 sources and sinks in multiple studies (e.g. Schoell, 1988; Whiticar, 1999). Stable isotope signatures can provide information on the processes responsible for CH_4 production and uptake as they are associated with a characteristic isotopic fractionation. The acetate fermentation pathway produces CH_4 depleted in deuterium (δD from − 400 to − 285‰) compared to the CO_2 reduction pathway (δD from − 250 to − 170‰) (Whiticar, 1999). Thermogenic CH_4 is typically enriched in ^{13}C whereas microbial CH_4 is typically depleted. When sulphate-reducing bacteria outcompete methanogens for acetate in marine sediments, CO_2 reduction becomes the main microbial pathway (Whiticar, 1999). More recently, aerobic pathways of CH_4 production from methylated compounds in oligotrophic oceanic waters have been reported (Karl et al., 2008; Damm et al., 2010). Sasakawa et al. (2008) reported $\delta^{13}C$ values up to + 5.9‰ in CH_4 emitted from sinking particles in subsurface seawater and attributed this strong enrichment to active microbial CH_4 oxidation occurring at anoxic/oxic boundaries present in these particles. Repeta et al. (2016) identified a new pathway, involving bacterial degradation of organic matter phosphonates, responsible for the production of CH_4 in aerobic surface waters. This process could resolve the marine CH_4 paradox, which refers to the ubiquitous CH_4 supersaturation in ocean surface waters, implying that methanogenesis occurs in the presence of oxygen. The $\delta^{13}C$ signatures of the CH_4 produced by this pathway are in the range of enriched values commonly measured in the ocean surface, from − 47 to − 44‰ (Repeta et al., 2016).

The purpose of this study was to measure, using high precision techniques, both isotopic signatures of CH_4 in surface waters of the Scheldt estuary, which is a well-studied environment located at the border between Belgium and the Netherlands. We illustrate how the co-isotopic tool can be applied to an estuarine environment to investigate dissolved CH_4 dynamics.

Study Location

From its source in northern France, the Scheldt spreads over 355 km in Belgium and the Netherlands before flowing into the North Sea. The catchment basin is densely populated with approximately 13 million inhabitants (Baeyens et al., 1998) and 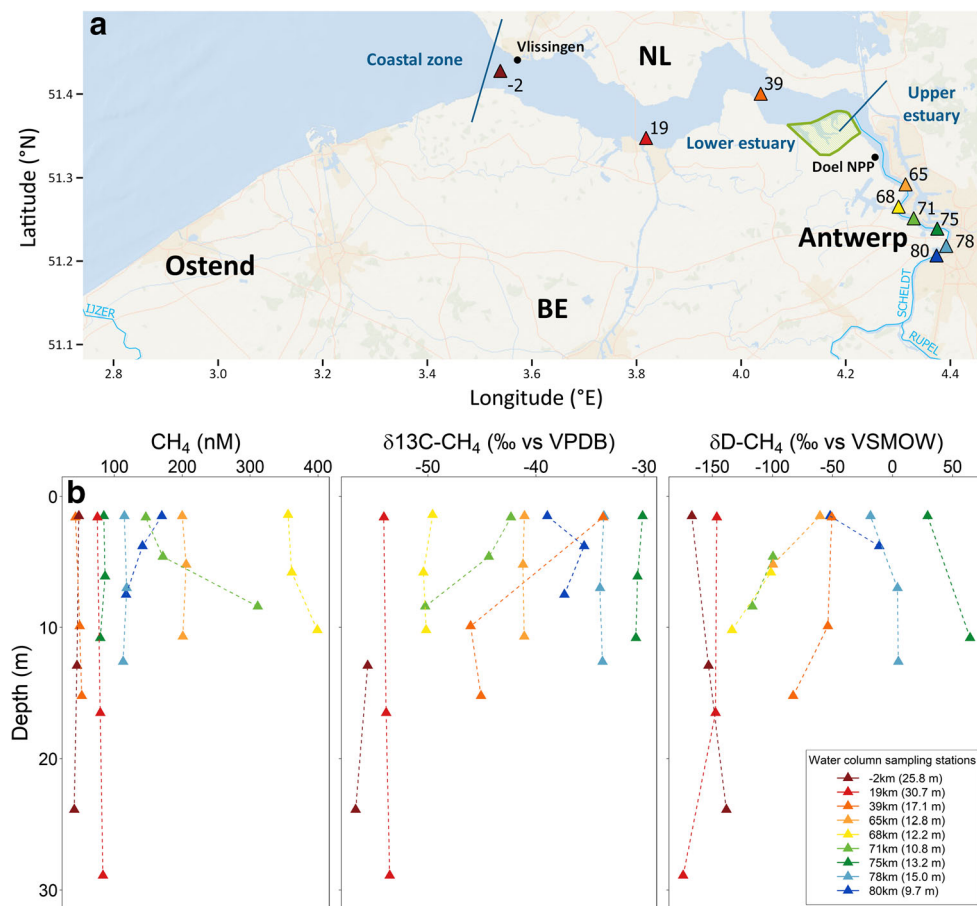is home to intense industrial and agricultural activities. The main city along the estuary is Antwerp whose port hosts several companies operating in the oil and chemical sector. A nuclear power plant composed of 4 nuclear reactors is located at Doel, downstream of the port area (Fig. 1a). For most of the twentieth century, wastewater originating mainly from Brussels was discharged in the river via the Rupel without further treatment, seriously deteriorating the water quality and leading to anoxia in the upper part of the estuary (Soetaert & Herman, 1995; Baeyens et al., 1998; Soetaert et al., 2006). Thanks to the implementation of an effective wastewater management plan in the 1980s, the water quality has gradually improved, with declining loads of total nitrogen and total phosphorus (Soetaert et al., 2006).

Given its hydrodynamical properties, the Scheldt estuary is conveniently divided into two zones (Baeyens et al., 1998). Taking the mouth of the estuary at Vlissingen as the 0 km reference point, the "lower estuary" extends up to 60 km upstream (at the Belgian-Dutch border) and is characterised by salinities typically comprised between 10 and 30. The "upper estuary" extends from 60 to 97 km (at the confluence of the Scheldt and the Rupel rivers), which includes the Port of Antwerp (Fig. 1a), and encompasses the zone of maximum turbidity, typically located at salinities between 2 and 10 (Baeyens et al., 1998). The location of the salinity transition between the upper and the lower estuary is not strict and varies with tides and river discharge. A dry period will result in an upstream shift (or salinity incursion), whereas a wet period will result in a downstream shift of this limit. Given the relatively low discharge of the Scheldt river (on average about 120 m³ s⁻¹), water exchange in the estuary is mostly governed by tides, leading to high residence times (months) and intense vertical mixing (Baeyens et al., 1998). Due to the large tidal range, the estuary is characterised by extensive intertidal areas, the greatest one being the brackish marsh of Saeftinghe, near the Belgian-Dutch border (green area in Fig. 1a).

Methods

Surface water was sampled at a total of 89 stations (numbered 1–49 and 100–139) starting from Ostend, at the Belgian coast, to Antwerp, following the rising tide, and back, on *RV Simon Stevin*, during fall 2015 and 2016 (8–9/12/2015 and 8–9/11/2016) (Fig. 2). The 2015 cruise reached the confluence between the Scheldt and the Rupel. During the 2016 cruise, the water column was also sampled at three depths (bottom, mid-depths and surface) at 9 stations (Fig. 1a and b). Water samples were collected using 60-mL borosilicate bottles, following established sampling protocols (Reeburgh, 2007; Borges et al., 2016): two bottles for concentration measurements and two bottles for isotope analyses. All samples were poisoned

Fig. 1 (**a**) Study area with the locations of the water column sampling stations, Doel nuclear power plant (Doel NPP) and the Saeftinghe marsh (green hatched area) and (**b**) vertical profiles of dissolved CH_4 in the water column of the Scheldt estuary in November 2016, labelled according to their distance in km from Vlissingen, with (left) concentration (nM), (middle) $\delta^{13}C$-CH_4 (‰ vs VPDB) and (right) δD-CH_4 (‰ vs VSMOW). Numbers in parentheses correspond to the water column depth

with $HgCl_2$ (1 µL mL^{-1}), closed with a butyl septum and an aluminium crimp seal and stored in the dark at ambient temperature until measurement. CH_4 concentrations were measured on a gas chromatograph (GC) equipped with a flame ionisation detector (FID), after headspace equilibration, as described in Borges et al. (2016). Raw data were corrected based on Upstill-Goddard et al. (1996) with Henry's constants from Yamamoto et al. (1976). The measurement precision estimated from sample duplicates is ± 2.2 nmol L^{-1}. Stable isotope analyses were conducted using a CH_4 preconcentration system coupled to a ThermoFinnigan Delta^{plus} XL isotope ratio mass spectrometer (Brass & Röckmann, 2010; Sapart et al., 2011). In each sample, 20 mL of He was injected to create a headspace and bottles were then vigorously shaken for 1 min and left to equilibrate for an hour as described in Sapart et al. (2017). The headspace was retrieved by addition of 20 mL of MilliQ water to the bottles and injected into a 40-mL sample loop. All δ values are reported in ‰ vs VPDB for $\delta^{13}C$ values and ‰ vs VSMOW for δD values. Precisions (1σ) for $\delta^{13}C$-CH_4 and δD-CH_4 measurements were ± 0.2‰ and ± 6.1‰, respectively. The standard deviation was calculated from reference air injections (Brass & Röckmann, 2010) for samples having similar concentrations.

Results

In December 2015, the dissolved CH_4 concentrations ranged between 15.9 and 94.7 nM in surface waters, with lowest values found in the upper estuary (Fig. 2a and Table S1). Saturation ratios were calculated with respect to CH_4 concentrations in equilibrium with an atmospheric mixing ratio of 1.9 ppm at *in situ* salinities and temperatures measured, following Wiesenburg and Guinasso (1979). Surface waters were supersaturated in CH_4 at all stations (Table S1), with supersaturation ratios ranging between 4.3 in the upper estuary and 28.6 in the lower estuary. The lower and upper parts of the estuary displayed distinct carbon isotopic signatures, from − 65.6 to − 51.4‰ and from − 44.7 to − 25.2‰, respectively (Fig. 2c). The signatures most enriched in heavy isotopes were measured near the confluence of the Scheldt river and the Rupel and in the Port of Antwerp, at salinities lower than 10. This spatial segregation was also apparent in the hydrogen isotopic signatures, with values ranging between − 212 and − 150‰ in the lower estuary and between − 64 and up to + 101‰ in the upper estuary (Fig. 2e).

In November 2016, on the contrary, the highest dissolved CH_4 concentrations in surface waters were measured in the upper estuary, with maximum values of 299.2 nM and
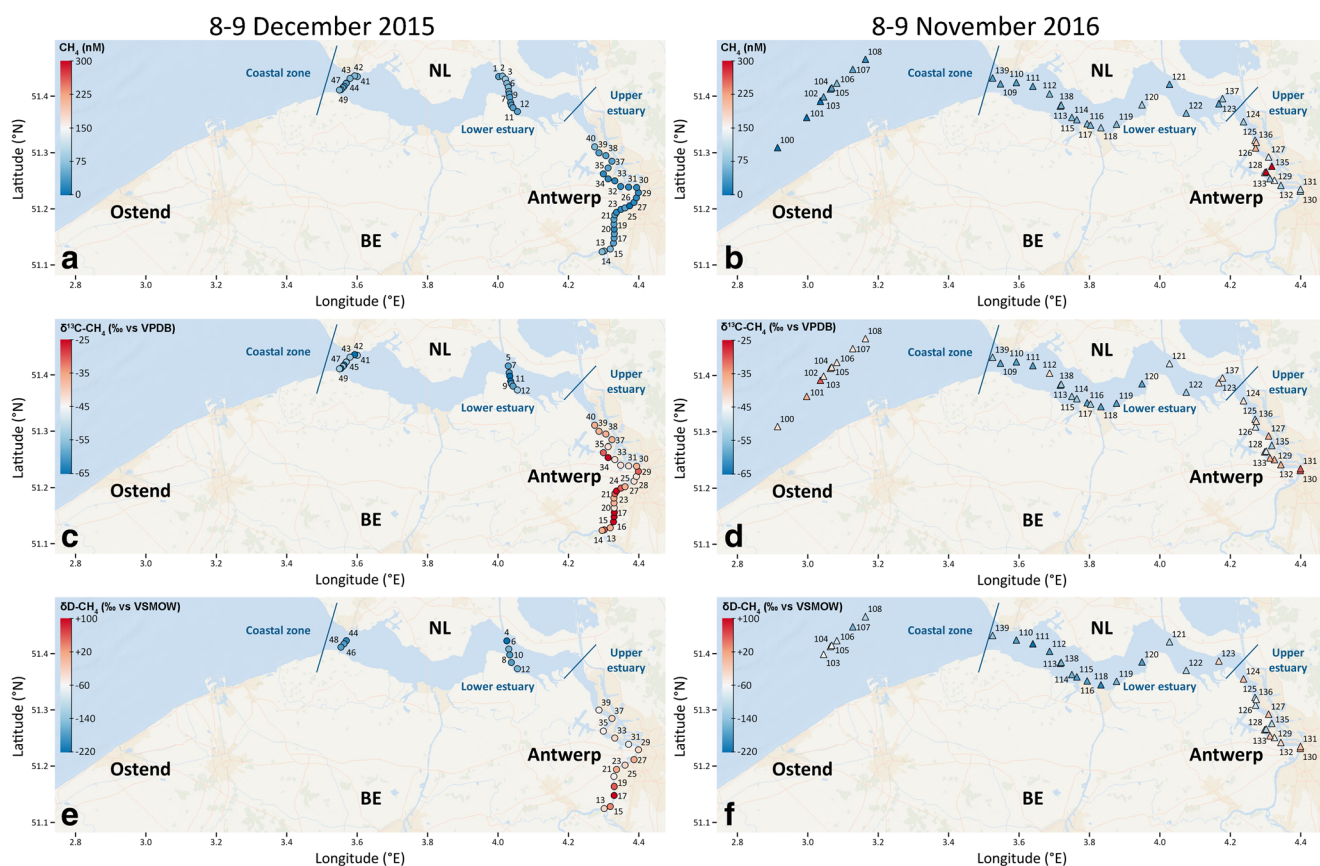
Fig. 2 Observed dissolved CH_4 concentrations (nM), $\delta^{13}C$-CH_4 (‰ vs VPDB) and δD-CH_4 (‰ vs VSMOW) in surface waters of the Scheldt estuary in December 2015 (**a**, **c**, **e**) and in November 2016 (**b**, **d**, **f**)

302.6 nM at stations 134 and 135, respectively (Fig. 2b). At the coastal stations and in the lower estuary, maximum concentrations reached 66.8 nM and 114.6 nM, respectively. Saturation ratios ranged from 5.3 to 94.2 (Table S1). As observed in December 2015, CH_4 was generally more depleted in heavy carbon isotopes in the lower estuary compared to the upper estuary where $\delta^{13}C$-CH_4 values up to -30.3‰ were measured (Fig. 2d). However, at coastal stations, CH_4 was also relatively enriched in heavy carbon isotopes, with $\delta^{13}C$-CH_4 values between -44.5 and -31.9‰. Hydrogen isotope signatures showed a similar pattern, with δD-CH_4 enriched in heavy isotopes up to -66.3‰ at coastal stations and up to $+6.7$‰ in the Port of Antwerp (Fig. 2f). In the water column, isotopic signatures amongst the most depleted in heavy isotopes were measured at stations "-2" and "19", whose depth profiles also show little change, possibly indicating good vertical mixing (lower estuary, Fig. 1b). Stations "39", "68" (where dissolved CH_4 concentrations reach 398.8 nM at the bottom) and "71" show evidence of upward diffusion of CH_4 from the sediments, associated with an isotopic enrichment towards the surface. Stations "65", "75" and "78" show interesting profiles, with little change in CH_4 concentrations and $\delta^{13}C$ signatures, but a sudden hydrogen isotope shift towards the surface. Very enriched carbon (up to -30.2‰) and

hydrogen (up to $+64.4$‰) isotopic signatures were measured at station "75" (upper estuary), along the depth profile. At station "80", dissolved CH_4 concentration decreased from the surface towards the riverbed, concurrent with an enrichment in heavy isotopes at mid-depth. A noticeable feature during the second cruise (November 2016) is an increase in water temperature by up to 2 °C when passing the Doel nuclear power plant, near stations 125 and 136 (Figure S1).
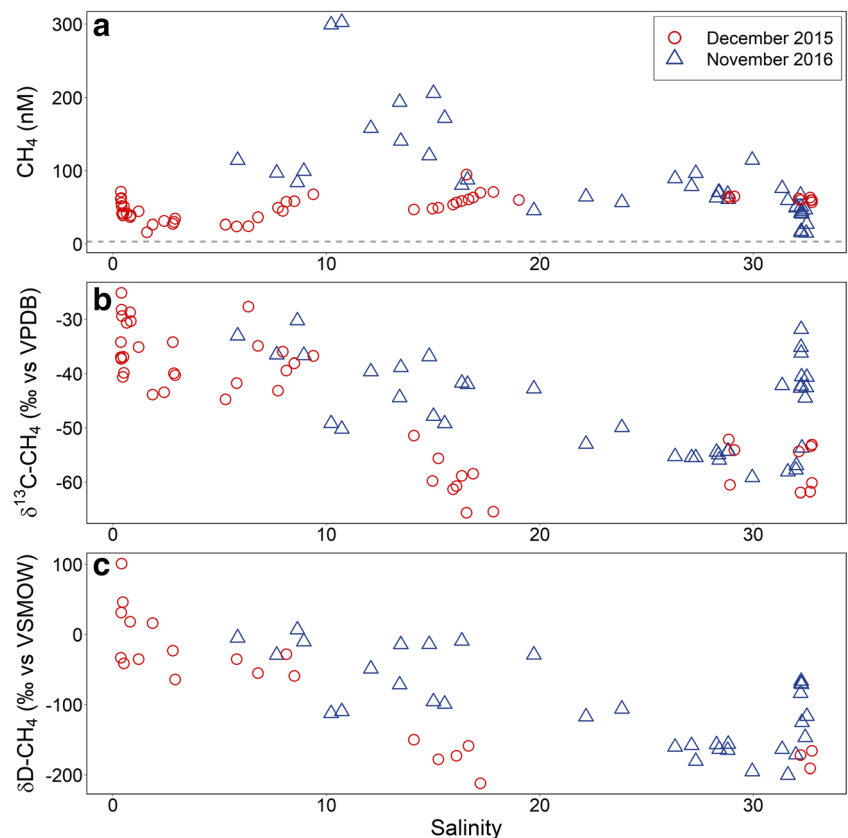
Discussion

During both cruises, CH_4 concentrations significantly exceeded equilibrium solubility, indicating that surface waters of the Scheldt estuary acted as a source of CH_4 to the atmosphere, consistent with prior work in this and other European estuaries (Middelburg et al., 2002; Upstill-Goddard & Barnes, 2016). The non-conservative behaviour of dissolved CH_4 along the salinity gradient in December 2015 and November 2016 (Fig. 3a) has been observed in other estuaries (Sansone et al., 1999) and points towards localised sources and sinks such as riverine inputs, methanogenesis in the riverbed and intertidal sediments, microbial oxidation and efflux to the atmosphere. In December 2015, a local minimum in CH_4

concentration was observed at salinities between 2 and 6. In November 2016, we lack freshwater end-member samples, but CH_4 concentrations decreased again upstream of the maximum observed at salinities around 10. Riverine CH_4 likely undergoes intense oxidation in the estuarine turbidity maximum (ETM), typically located at these salinities, as highlighted in Abril et al. (2007). Unfortunately, we did not measure suspended particulate matter (SPM) concentrations that would support this hypothesis. In November 2016, CH_4 concentrations reached maximum values (up to 302.6 nM) at intermediate salinities. Such a local maximum (also observed at salinities between 5 and 10 in Middelburg et al. (2002) during May, June, October and December) is present, but to a lower extent (67.5 nM), in our December 2015 data set and might be attributed to CH_4 formation from localised peaty sediments in the Port of Antwerp (Baeyens et al., 1998). Vertical profiles of CH_4 at stations "68" and "71" show highest concentrations towards the sediment, progressively decreasing towards the surface, in agreement with this hypothesis (Fig. 1b). Dissolved CH_4 concentrations are subject to large temporal variability, given the influence of physical environmental factors such as tidal mixing and river discharge, as illustrated by the differences in surface concentrations between both years (Fig. 3a). For example, falling tides influence the concentration of CH_4 by exerting a lower hydrostatic pressure on sediments, favouring the release of CH_4 bubbles accumulated in

pore waters due to the low solubility of the gas (Chanton et al., 1989; Middelburg et al., 1996). At low tide, the upward migration of gas bubbles in the shallow water column is fast, reducing the gas exposure to microbial oxidation, i.e. it bypasses the microbial CH_4 consumption zone. Conversely, bubble production and release are suppressed at high tide, which also increases CH_4 exposure to microbial oxidation and further reduces the amount of CH_4 emitted to the atmosphere. River discharge and subsequent mixing with seawater will also influence dissolved CH_4 concentrations in the estuary (de Angelis & Lilley, 1987). According to the Belgian Royal Meteorological Institute (RMI), precipitation was abnormally low in September 2016, leading to a low river discharge in fall 2016 (Maris & Meire, 2017), likely explaining the salinity intrusion in the upper estuary in November 2016 (Figure S2), and the shift of the local CH_4 maximum to salinities between 10 and 15 (Fig. 3a).

Stable isotope analysis can represent a powerful tool to determine the origin of CH_4 in aquatic environments (e.g. Schoell, 1988; Whiticar, 1999), because of the characteristic isotopic fractionation associated with CH_4 production and consumption pathways. The pattern of $\delta^{13}C$ and δD along the salinity gradient was similar for both years (Fig. 3b and c). We observe a gradual shift from signatures enriched in heavy isotopes at low salinities (the upper estuary) to depleted

Fig. 3 Evolution of (a) dissolved CH_4 concentrations (nM), (b) $\delta^{13}C$-CH_4 (‰ vs VPDB) and (c) δD-CH_4 (‰ vs VSMOW) with salinity in surface waters of the Scheldt estuary in December 2015 (red circles) and November 2016 (blue triangles). The grey dashed line represents the range of equilibrium solubilities (2.8–3.8 nM) calculated for the temperatures and salinities measured during both cruises and with an atmospheric mixing ratio of 1.9 ppm

signatures at higher salinities (lower estuary), followed by an enrichment at the mouth of the estuary and the coastal area.

We also report our isotopic data on a dual isotope plot (Fig. 4). They show a linear trend and fit in between and above the three domains defined by Whiticar (1999) for the main CH_4 production pathways: acetate fermentation, CO_2 reduction and thermogenic degradation. Isotopic values that are so enriched in both heavy isotopes (up to $-25.2‰$ for $\delta^{13}C$ and $+101‰$ for δD) are quite unusual. The gradual depletion of isotopic signatures from the upper estuary to the mouth could indicate an increasing contribution of microbial CH_4 production, likely originating from the mineralisation of locally produced organic matter (Middelburg et al., 1996). The lower estuary indeed harbours extensive intertidal flats and marshes, known to release CH_4 (Middelburg et al., 1996, 2002). The reasons behind the unusually enriched isotopic signatures measured in the upper estuary however remain unclear.
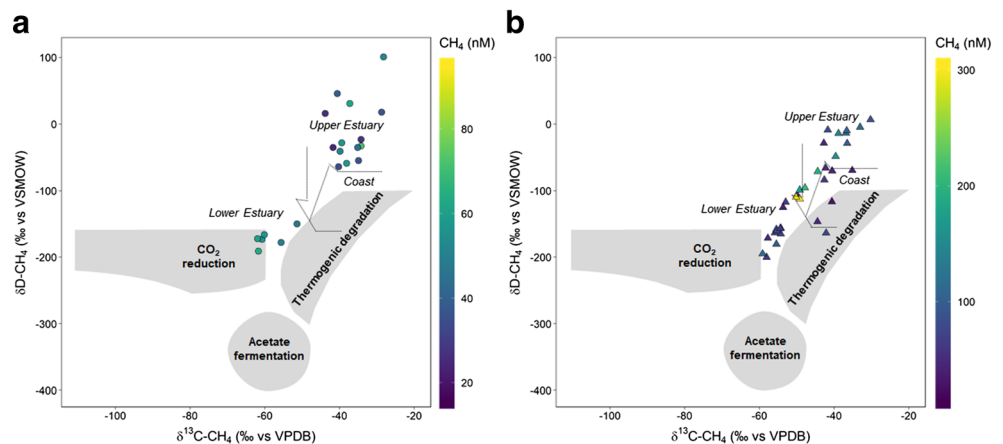
The linear array of $\delta^{13}C$ and δD in Fig. 4 could also possibly reflect an increasing contribution of closed system microbial oxidation modifying a single source signal. This would occur in case methanotrophs are active, since these preferentially consume lighter CH_4, leaving the remaining pool more enriched in both heavy isotopes. An extreme case of that process could lead to the unusually high isotopic values observed in the upper estuary. However, in the case of a simple closed system, the isotopic enrichment due to oxidation should be accompanied by CH_4 consumption and therefore a decrease in CH_4 concentration, which is clearly not observed for the whole Scheldt estuary data set of Fig. 4. This would confirm that local CH_4 sources and sinks play a key role in this complex system, evolving far from a single source-closed system.

Sansone et al. (1999) observed a wide range of isotopic signatures in five American estuaries, with $\delta^{13}C$ values as enriched as $-36.2‰$ in freshwater end-members, and values as depleted as $-60.4‰$ at the mouth. Unfortunately, δD was not measured in their study. To our best knowledge, our work is the first to measure both CH_4 isotopic signatures in an estuary, at high spatial resolution, and to report such enriched values. Few studies report extremely positive values for δD-CH_4 from gas seeps (Etiope et al., 2011; Daskalopoulou et al., 2018; Milkov & Etiope, 2018), but this has never been observed in estuarine environments. In order to investigate whether microbial oxidation alone could lead to isotopic signatures as enriched as the ones we measured in the upper estuary, we plotted all (surface and profiles) our $\delta^{13}C$ and δD data as a function of the logarithm of their CH_4 concentration in Fig. 5a and b, respectively. We grouped the stations by zone and by year and calculated linear regressions (Table 1).

The best fit ($R^2 = 0.78$ for $\delta^{13}C$ and 0.83 for δD), obtained for upper estuary stations in November 2016 (dark blue triangles in Fig. 5b), indicates that the low river discharge encountered that year, created particular conditions that could be approximated by a closed system, where dissolved CH_4 is consumed by a single sink. According to the Rayleigh fractionation model, the slope of this relationship can be used to derive isotopic fractionation factors (ε) of $12.8‰$ and $100.8‰$ for carbon and hydrogen, respectively. Conversely, we attribute the weak correlations obtained in December 2015 and in the lower estuary in November 2016, to the fact that a single process (e.g. microbial oxidation) does not dominate the CH_4 dynamics but rather a combination of processes. This demonstrates the limitation of applying the Rayleigh approach to our data set, since the basic assumption of single source-closed system conditions is not satisfied. Nevertheless, this interpretation qualitatively illustrates how concentration and isotope signatures are expected to co-evolve due to oxidation, and allows investigating whether this oxidation could be responsible for such unexpected observed isotopic signatures, at least for part of the data set. Moreover, the deduced ε values fall within the ranges that are expected from previous investigations in the literature. To our knowledge, only one study reports fractionation factors associated with CH_4 oxidation in estuaries, with ε_C values ranging from 4.2 to 12‰ (Sansone et al., 1999). The range of ε_C and ε_D values attributed to

Fig. 4 Dissolved CH_4 concentrations (nM) in surface waters of the Scheldt estuary in December 2015 (a) and November 2016 (b), reported on a dual isotope plot together with the typical isotopic composition of oceanic CH_4 sources, adapted from Whiticar (1999) and delimited by locations (see Fig. 1). Note the different concentration scales
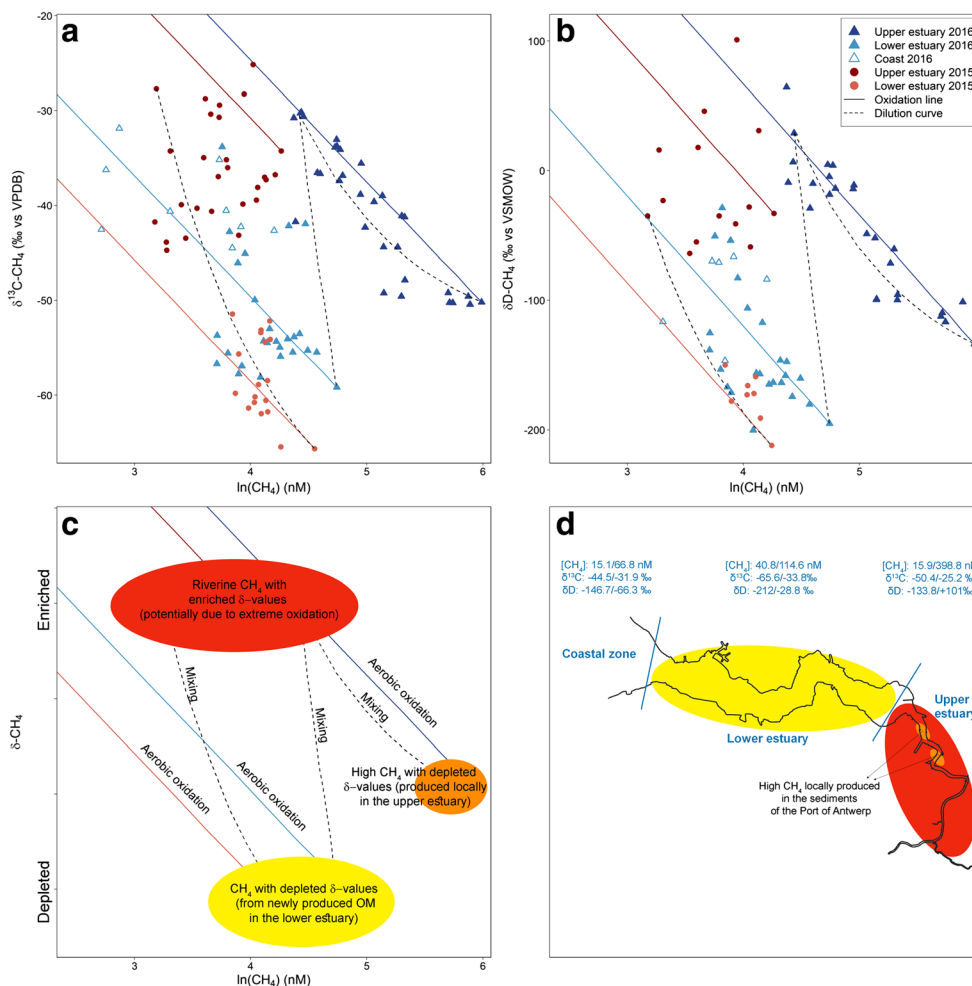
Fig. 5 Carbon (**a**) and hydrogen (**b**) isotopic signatures plotted as a function of the logarithm of dissolved CH_4 concentrations measured in the Scheldt estuary. We grouped the stations by zone and by year and calculated linear regressions. The best fit ($R^2 = 0.78$ for $\delta^{13}C$ and 0.83 for δD) was obtained for upper estuary stations in November 2016 (dark blue triangles). Following the Rayleigh fractionation approach, we used the slope of this relationship to derive isotopic fractionation factors (ε) of 12.8‰ and 100.8‰ for C and H respectively, that we applied to the more concentrated values in each zone to obtain theoretical oxidation lines

(solid lines). We also drew a few exemplative mixing curves (dashed lines) between extreme end-members within each year, to illustrate the impact of this potential process on the data distribution. Panel (**c**) identifies the various pools of CH_4 associated with characteristic isotopic signatures in the estuary and the processes potentially influencing these values. Panel (**d**) summarises the range of dissolved CH_4 concentrations and isotopic signatures measured in the coastal area, the upper and the lower estuary, and locates the three main pools of CH_4 identified in this study

anaerobic oxidation of CH_4 in coastal sediments is typically of 8–12‰ and 100–180‰, respectively (e.g. Alperin & Reeburgh, 1988; Martens et al., 1999). The isotopic fractionation induced by aerobic oxidation measured in laboratory

incubations ranges from 13 to 26 ‰ for carbon and from 97 to 350‰ for hydrogen (Coleman et al., 1981).

Based on our best fit estimates of ε_C and ε_D for the upper estuary stations in November 2016, theoretical oxidation lines

Table 1 Correlation coefficients of the linear regressions performed on the relationship between the δ signatures and the logarithm of their concentrations, in the upper and lower part of the estuary, in December 2015 and November 2016

Year	Zone	R^2 $\delta^{13}C$ vs ln (CH_4)	R^2 δD vs ln (CH_4)
December 2015	Lower estuary	0.20	0.51
	Upper estuary	0.04	0.01
November 2016	Lower estuary with coastal stations	0.36	0.30
	Lower estuary without coastal stations	0.06	0.33
	Upper estuary	0.78	0.83

were drawn taking the highest CH_4 concentration in each group, as the initial value (Fig. 5a and b). This extrapolation to the lower estuary and to the December 2015 data set allows investigating the influence of microbial oxidation on potential CH_4 sources, surmising fractionation factors were constant in time and space. In November 2016, the oxidation line reproduces quite well the pattern observed for upper estuary stations, implying that in theory, aerobic oxidation has the potential to lead to $\delta^{13}C$ and δD values as enriched as $-30.3‰$ and $+64.4‰$, respectively. These enriched signatures coincide with very low remaining fractions of dissolved CH_4 (< 0.2). This implies that either the observed signatures are inherited from upstream riverine oxidation processes or that 80% of the CH_4 produced by the mineralisation of organic matter in the upper estuary would need to be oxidised despite the low exposure time induced by the shallow water column at that location. This is in agreement with the findings of de Angelis and Scranton (1993) and Abril and Iversen (2002) who showed that oxidation rates are particularly high in the upper part of an estuary, at low salinities. This can be attributed to a salinity effect on methanotrophic activity (de Angelis & Scranton, 1993; Osudar et al., 2015; Osudar et al., 2017) and to the relative high biomass of nitrifying and methanotrophic bacteria in estuarine turbidity zones in the upper estuary (Owens, 1986; Abril et al., 2000; Abril et al., 2007). In any case, the origin of riverine CH_4 highly enriched in heavy isotopes (our first option) is still conjectural and cannot be resolved with our current data set. Reasonable assumptions include methanogenesis from highly oxidised organic matter, aerobic oxidation of CH_4 produced upstream or groundwater discharge, which can carry dissolved CH_4 quite enriched in heavy isotopes (Vigneron et al., 2017). Additional sampling upstream is required to investigate these hypotheses.

Except for the upper estuary in November 2016, the potential oxidation lines drawn in Fig. 5a and b for the other groups only explain part of the data distribution, implying that other processes are at stake. In this very dynamic estuarine system, mixing between dissolved CH_4 molecules produced at different locations and at different stages of oxidation should also be considered. With this in mind, we drew a few exemplative dilution curves between extreme end-members to illustrate the impact of this process on the data distribution and how it would blur the simplistic trend attributed to aerobic oxidation (dashed lines, Fig. 5a and b). In the specific case of upper estuary stations in November 2016, the dilution curve reproduces well the dispersion of the observed distribution (dark blue triangles in Fig. 5a and b). This study identifies three potential dissolved CH_4 pools with distinct isotopic signatures (Fig. 5c): riverine CH_4 with surprisingly enriched δ values (red ellipse), highly concentrated CH_4 with depleted δ values produced locally in the sediments of the Port of Antwerp (orange ellipse), and CH_4 with depleted δ values from newly produced organic matter in the lower estuary (yellow ellipse).

The concurrent action of aerobic oxidation and mixing therefore supports the wide range of isotopic signatures and concentrations measured in this study. Figure 5d summarises these ranges in each zone and highlights the spatial prevalence of each CH_4 pool in the lower and upper parts of the estuary.

Finally, it is worth noting the special case of the coastal stations. These are located in an area where high dissolved CH_4 concentrations were reported due to the presence of gassy sediments (Borges et al., 2016). Based on the enriched signatures we measured in surface waters of this area, the origin of the CH_4 could be either thermogenic or microbial with a longer exposure to oxidation due to the increase in water column depth. The first option is supported by the position of some of the coastal samples in Fig. 4b. The latter option cannot be confirmed by the limited coastal data set in Fig. 5a and b. Further sampling above the sediments and in the water column for concentration and isotopic analyses will help identify the origin of this CH_4 enriched in heavy isotopes.

Conclusion

Our data confirm literature reports of very high and variable dissolved CH_4 concentrations in the Scheldt estuary. We have complemented these measurements with a unique data set of both CH_4 stable isotopes ($\delta^{13}C$ and δD). We show that CH_4 dissolved in the upper estuary is unusually enriched in ^{13}C and D and results either from an intense aerobic oxidation in the upper estuary, an unknown upstream source or both. This enriched CH_4 is further exposed to aerobic oxidation along the estuary and undergoes mixing with depleted CH_4 produced by methanogenesis in the sediments, before entering the North Sea. Complex biogeochemical models should be used at a later stage to refine the analysis and more strictly quantify the processes identified in this study. To further investigate the estuarine CH_4 cycling, we recommend additional water sampling upstream to characterise the contribution of riverine input to the enriched signatures measured at salinities close to 0. We further recommend that future studies also include atmospheric and flux measurements in order to better understand the role of the estuary in terms of CH_4 emissions. Our observed CH_4 isotope anomalies in the Scheldt estuary highlight that important unknowns remain to be resolved for the estuarine CH_4 cycle.

thank Profs. F. Fripiat and S. Arndt for their precious advice, as well as the two anonymous referees for their constructive comments.

References

Abril, G., & Borges, A. V. (2004). Carbon dioxide and methane emissions from estuaries. In A. Tremblay, L. Varfalvy, C. Roehm, & M. Garneau (Eds.), *Greenhouse gas emissions: fluxes and processes, hydroelectric reservoirs and natural environments.* (pp. 187–207). https://doi.org/10.1007/3-540-26643-7_7.

Abril, G., M.V. Commarieu, and F. Guérin. 2007. Enhanced methane oxidation in an estuarine turbidity maximum. *Limnology and Oceanography* 52 (1): 470–475. https://doi.org/10.4319/lo.2007.52.1.0470.

Abril, G., and N. Iversen. 2002. Methane dynamics in a shallow non-tidal estuary (Randers Fjord, Denmark). *Marine Ecology Progress Series* 230: 171–181. https://doi.org/10.3354/meps230171.

Abril, G., S.A. Riou, H. Etcheber, M. Frankignoulle, R. De Wit, and J.J. Middelburg. 2000. Transient, tidal time-scale, nitrogen transformations in an estuarine turbidity maximum - fluid mud system (the Gironde, South-West France). *Estuarine, Coastal and Shelf Science* 50 (5): 703–715. https://doi.org/10.1006/ecss.1999.0598.

Alperin, M.J., and W.S. Reeburgh. 1988. Carbon and hydrogen isotope fractionation resulting from anaerobic methane oxidation. *Global Biogeochemical Cycles* 2 (3): 279–288.

Baeyens, W., B. Van Eck, and C. Lambert. 1998. General description of the Scheldt estuary. *Hydrobiologia* 366: 1–14.

Borges, A.V., W. Champenois, N. Gypens, B. Delille, and J. Harlay. 2016. Massive marine methane emissions from near-shore shallow coastal areas. *Scientific Reports* 6 (1): 27908. https://doi.org/10.1038/srep27908.

Brass, M., and T. Röckmann. 2010. Continuous-flow isotope ratio mass spectrometry method for carbon and hydrogen isotope measurements on atmospheric methane. *Atmospheric Measurement Techniques* 3 (6): 1707–1721. https://doi.org/10.5194/amt-3-1707-2010.

Chanton, J.P., C.S. Martens, and C.A. Kelley. 1989. Gas transport from methane-saturated, tidal freshwater and wetland sediment. *Limnology* 34 (5): 807–819.

Coleman, D.D., J.D. Risatti, and M. Schoell. 1981. Fractionation of carbon and hydrogen isotopes by methane-oxidising bacteria. *Geochimica et Cosmochimica Acta* 45 (7): 1033–1037.

Damm, E., E. Helmke, S. Thoms, U. Schauer, E. Nöthig, K. Bakker, and R.P. Kiene. 2010. Methane production in aerobic oligotrophic surface water in the central Arctic Ocean. *Biogeosciences Discussions* 6 (6): 10355–10379. https://doi.org/10.5194/bgd-6-10355-2009.

Daskalopoulou, K., S. Calabrese, F. Grassa, K. Kyriakopoulos, F. Parello, F. Tassi, and W. D'Alessandro. 2018. Origin of methane and light hydrocarbons in natural fluid emissions: a key study from Greece. *Chemical Geology* 479 (August 2017): 286–301. https://doi.org/10.1016/j.chemgeo.2018.01.027.

de Angelis, M.A., and M.D. Lilley. 1987. Methane in surface waters of Oregon estuaries and rivers. *Limnology and Oceanography;(USA)* 32 (3): 716–722. https://doi.org/10.4319/lo.1987.32.3.0716.

de Angelis, Marie A., and M.I. Scranton. 1993. Fate of methane in the Hudson river and estuary. *Global Biogeochemical Cycles* 7 (3): 509–523.

Etiope, G., C.L. Baciu, and M. Schoell. 2011. Extreme methane deuterium, nitrogen and helium enrichment in natural gas from the Homorod seep (Romania). *Chemical Geology* 280 (1–2): 89–96. https://doi.org/10.1016/j.chemgeo.2010.10.019.

Karl, D.M., L. Beversdorf, K.M. Björkman, M.J. Church, A. Martinez, and E.F. Delong. 2008. Aerobic production of methane in the sea. *Nature Geoscience* 1 (7): 473–478. https://doi.org/10.1038/ngeo234.

Maris, T., & Meire, P. (2017). Onderzoek naar de gevolgen van het Sigmaplan, baggeractiviteiten en havenuitbreiding in de Zeeschelde op het milieu.

Martens, C.S., D.B. Albert, and M.J. Alperin. 1999. Stable isotope tracing of anaerobic methane oxidation in the gassy sediments of Eckernförde Bay, German Baltic Sea. *American Journal of Science* 299 (7-9): 589–610. https://doi.org/10.2475/ajs.299.7-9.589.

Middelburg, J.J., G. Klaver, J. Nieuwenhuize, A. Wielemaker, W. De Haas, T. Vlug, and J.F.W.A. Van Der Nat. 1996. Organic matter mineralization in intertidal sediments along an estuarine gradient. *Marine Ecology Progress Series* 132 (1–3): 157–168. https://doi.org/10.3354/meps132157.

Middelburg, J. J., Nieuwenhuize, J., Iversen, N., Høgh, N., De Wilde, H., Helder, W., … Christof, O. (2002). Methane distribution in European tidal estuaries. Biogeochemistry, 59(1–2), 95–119. https://doi.org/10.1023/A:1015515130419.

Milkov, A.V., and G. Etiope. 2018. Organic geochemistry revised genetic diagrams for natural gases based on a global dataset of >20,000 samples. *Organic Geochemistry* 125: 109–120. https://doi.org/10.1016/j.orggeochem.2018.09.002.

Osudar, R., K.W. Klings, D. Wagner, and I. Bussmann. 2017. Effect of salinity on microbial methane oxidation in freshwater and marine environments. *Aquatic Microbial Ecology* 80 (2): 181–192. https://doi.org/10.3354/ame01845.

Osudar, R., A. Matoušů, M. Alawi, D. Wagner, and I. Bussmann. 2015. Environmental factors affecting methane distribution and bacterial methane oxidation in the German Bight (North Sea). *Estuarine, Coastal and Shelf Science* 160: 10–21. https://doi.org/10.1016/j.ecss.2015.03.028.

Owens, N.J.P. 1986. Estuarine nitrification: a naturally occurring fluidized bed reaction? *Estuarine, Coastal and Shelf Science* 22 (1): 31–44. https://doi.org/10.1016/0272-7714(86)90022-3.

Reeburgh, W. 2007. Oceanic methane biogeochemistry. *American Chemical Society* 107 (2): 486–513. https://doi.org/10.1021/cr050362v.

Repeta, D.J., S. Ferrón, O.A. Sosa, C.G. Johnson, L.D. Repeta, M. Acker, E.F. DeLong, and D.M. Karl. 2016. Marine methane paradox explained by bacterial degradation of dissolved organic matter. *Nature Geoscience* 9 (12): 884–887. https://doi.org/10.1038/ngeo2837.

Sansone, F.J., M.E. Holmes, and B.N. Popp. 1999. Methane stable isotopic ratios and concentrations as indicators of methane dynamics in estuaries. *Global Biogeochemical Cycles* 13 (2): 463–474. https://doi.org/10.1029/1999GB900012.

Sapart, C. J., Van Der Veen, C., Vigano, I., Brass, M., Van De Wal, R. S. W., Bock, M., … Röckmann, T. (2011). Simultaneous stable isotope analysis of methane and nitrous oxide on ice core samples. Atmospheric Measurement Techniques, 4(12), 2607–2618. https://doi.org/10.5194/amt-4-2607-2011.

Sapart, Célia J, Shakhova, N., Semiletov, I., Jansen, J., Szidat, S., Kosmach, D., …, Röckmann, T. (2017). The origin of methane in the East Siberian Arctic Shelf unraveled with triple isotope analysis. *Biogeosciences Discussions*, 1–22. https://doi.org/10.5194/bg-2016-367

Sasakawa, M., Tsunogai, U., Kameyama, S., Nakagawa, F., Nojiri, Y., & Tsuda, A. (2008). Carbon isotopic characterization for the origin of excess methane in subsurface seawater. Journal of Geophysical Research: Oceans, 113(3). https://doi.org/10.1029/2007JC004217.

Schoell, M. 1988. Multiple origins of methane in the earth. *Chemical Geology* 71 (1–3): 1–10. https://doi.org/10.1016/0009-2541(88)90101-5.

Scranton, M.I., and K. McShane. 1991. Methane fluxes in the southern North Sea: the role of European rivers. *Continental Shelf Research* 11 (1): 37–52. https://doi.org/10.1016/0278-4343(91)90033-3.

Soetaert, K., and P.M.J. Herman. 1995. Estimating estuarine residence times in the Westerschelde (The Netherlands) using a box model with fixed dispersion coefficients. *Hydrobiologia* 311 (1-3): 215–224. https://doi.org/10.1007/BF00008582.

Soetaert, Karline, J.J. Middelburg, C. Heip, P. Meire, S. Van Damme, and T. Maris. 2006. Long-term change in dissolved inorganic nutrients in the heterotrophic Scheldt estuary. *Limnology and Oceanography* 51 (1part2): 409–423.

Upstill-Goddard, R.C., and J. Barnes. 2016. Methane emissions from UK estuaries: re-evaluating the estuarine source of tropospheric methane from Europe. *Marine Chemistry* 180: 14–23. https://doi.org/10.1016/j.marchem.2016.01.010.

Upstill-Goddard, R.C., A.P. Rees, and N.J.P. Owens. 1996. Simultaneous high-precision measurements of methane and nitrous oxide in water and seawater by single phase equilibration gas chromatography. *Deep Sea Research Part I* 43 (10): 1669–1682.

Vigneron, A., Bishop, A., Alsop, E. B., Hull, K., Rhodes, I., Hendricks, R., … Tsesmetzis, N. (2017). Microbial and isotopic evidence for methane cycling in hydrocarbon-containing groundwater from the Pennsylvania region. Frontiers in Microbiology, 8(APR), 1–12. https://doi.org/10.3389/fmicb.2017.00593.

Whiticar, M.J. 1999. Carbon and hydrogen isotope systematics of bacterial formation and oxidation of methane. *Chemical Geology* 161 (1–3): 291–314.

Wiesenburg, D.A., and N.L. Guinasso Jr. 1979. Equilibrium solubilities of methane, carbon monoxide, and hydrogen in water and sea water. *Journal of Chemical & Engineering Data* 24 (4): 356–360. https://doi.org/10.1021/je60083a006.

Yamamoto, S., J.B. Alcauskas, and T.E. Crozier. 1976. Solubility of methane in distilled water and sea water. *Journal of Chemical and Engineering Data* 21 (1): 78–80. https://doi.org/10.1021/je60068a029.